INTERNATIONAL JOURNAL OF AUTOMOTIVE SCIENCE AND TECHNOLOGY

2026, VOL. 10, NO:3, 692-710 www.ijastech.org e-ISSN: 2587-0963

A Comprehensive Review of Battery State of Health Estimation: Methods, Challenges and Future Perspectives

Hakan Çoban[1*], Koray Erhan[2] and Mustafa Baysal[1]

[1.] *Department of Electrical Engineering, Faculty of Electrical and Electronics, Yıldız Technical University, Istanbul, 34220, Turkey*
[2.] *Department of Mechatronics Engineering, Faculty of Technology, Marmara University, Istanbul, 34854, Turkey*

Abstract

Lithium-ion battery state of health (SOH) cannot be measured directly and must be inferred from capacity, resistance, voltage, current, temperature, and usage history. This structured narrative review integrates degradation mechanisms with feature-based, model-based, data-driven, and physics -informed/hybrid estimation methods, and evaluates them against validation design, chemistry dependence, uncertainty, computational burden, and on-board feasibility. The literature was updated through targeted searches of Crossref-indexed publisher platforms, IEEE Xplore, ScienceDirect, SpringerLink/Nature, Wiley Online Library, and MDPI; 117 unique publications, institutional reports, and regulatory documents were retained after duplicate removal and relevance screening. Reported errors are treated as study-specific results rather than universal characteristics of method families. The synthesis shows that no single estimator is uniformly superior: feature-based diagnostics provide physical insight but require informative and low-noise operating segments; equivalent-circuit observers are compatible with embedded implementation but depend on model adaptation; data-driven models can achieve low error within their validation domain but require rigorous cross-cell and cross-condition testing; and physics-informed or hybrid approaches offer a promising compromise when their added complexity is justified. Future progress depends on transparent validation, uncertain-aware estimation, chemistry transfer, compact edge implementation, multimodal sensing, and auditable life-cycle data under emerging battery regulations.

Keywords: State of Health (SOH); lithium-ion batteries; battery management system (BMS); validation; uncertainty quantification; machine learning

Review Article

History
Received 15.06.2026
Revised 17.09.2026
Accepted 01.10.2026

Contact
* Corresponding author
Hakan Çoban
hakann.cobann@gmail.com
Address: Electrical Engineering Department, Faculty of Electrical and Electronics, Yıldız Technical University, Istanbul, Turkey
Tel:+902123835800

To cite this paper: Çoban, H., Erhan, K., Baysal, M. A Comprehensive Review of Battery State of Health Estimation: Methods, Challenges and Future Perspectives. International Journal of Automotive Science and Technology. 2026; 10(3), 692-710 https://doi.org/10.30939/ijastech..1995891

1. Introduction

Lithium-ion batteries are central to electric mobility and stationary energy storage because they combine high specific energy, high round-trip efficiency, and long cycle life. Their performance nevertheless evolves with time and use, and this evolution depends on chemistry, cell design, temperature, state-of-charge window, current rate, storage history, and mechanical loading [1-4]. Battery management systems therefore require state estimates that remain reliable under partial charging, dynamic current profiles, sensor limitations, and cell-to-cell variability.

Battery state of health (SOH) is a latent indicator of the departure from beginning-of-life performance. Capacity-based SOH tracks the maximum available charge, whereas resistance- or power-based SOH represents the loss of power capability associated with impedance growth [5, 6]. Because the selected definition changes the numerical value and the end-of-life decision, every study should state the reference quantity, test conditions, and threshold explicitly.

$$SOH_C = \frac{C_{now} - C_{EOL}}{C_{nominal} - C_{EOL}} * 100\% \quad (1)$$

$$SOH_R = \frac{R_{EOL} - R_{now}}{R_{EOL} - R_{nominal}} * 100\% \quad (2)$$

Equation (1) defines a capacity-normalized health index and Equation (2) defines a resistance-normalized health index. C_now is the measured maximum available capacity at the current age (Ah), C_nominal is the beginning-of-life or rated capacity (Ah), and C_EOL is the application-specific end-of-life capacity (Ah). R_now is the present internal resistance (Ω), R_nominal is the beginning-of-life resistance (Ω), and R_EOL is the application-specific end-of-life

resistance (Ω). With these normalized definitions, 100% denotes beginning of life and 0% denotes the selected end-of-life (EOL) threshold. Automotive capacity thresholds are commonly located near 70-80% of initial capacity, but they are application- and manufacturer-dependent rather than universal [6, 7].

Battery aging arises from coupled electrochemical and mechanical processes. Solid-electrolyte-interphase growth and lithium plating contribute to loss of lithium inventory, while particle cracking, phase change, and loss of electrical contact contribute to loss of active material and resistance increase [5, 8-10]. Temperature, C-rate, depth of discharge, average SOC, rest periods, and load history alter both the dominant mechanism and its rate. SOH is therefore not directly measurable from a single terminal signal; it must be inferred from observable quantities under a stated model and validation protocol. Figure 1 summarizes this life-cycle interpretation and the application-dependent transition from first-life operation to evaluation for reuse, repurposing, or recycling. It is an illustration synthesized by the authors from the degradation, prognostics, and second-life literature cited above rather than a plot of a single experimental dataset, and the thresholds it shows are application-dependent.

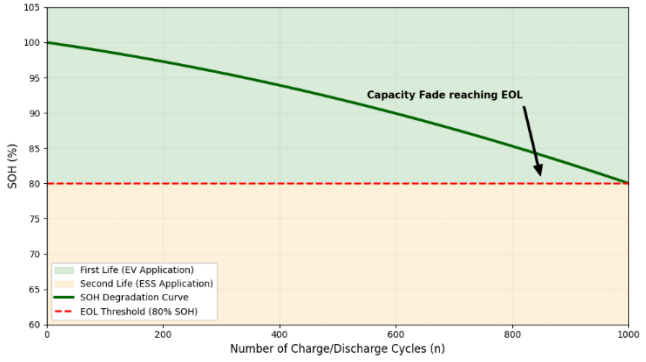


Figure 1. Conceptual battery SOH life-cycle framework (authors' illustration, [5, 6, 11, 12]).

Accurate and auditable SOH information supports warranty decisions, residual-value assessment, second-life screening, and recycling logistics. Regulation (EU) 2023/1542 introduces information, performance, durability, and battery-passport requirements on staged implementation dates; it does not establish a universal SOH threshold for every second-life decision. Consequently, technical screening must combine SOH with safety history, fault information, cell imbalance, and the requirements of the intended second-life duty [11, 12].

This review connects four estimator families — feature-based, model-based, data-driven, and physics-informed/hybrid methods — to degradation mechanisms, chemistry-dependent observability, validation design, uncertainty, embedded implementation, and life-cycle regulation. Unlike reviews focused primarily on one algorithm family, it uses a deployment-oriented question: which evidence is required before a reported laboratory result can be interpreted as suitable for an on-board battery management system (BMS) or fleet-level application?

1.1. Review Methodology

This article is a structured narrative review, not a PRISMA-style systematic review or meta-analysis. The search was updated on 27 August 2026 using Crossref-indexed publisher records and targeted searches in IEEE Xplore, ScienceDirect, SpringerLink/Nature, Wiley Online Library, and MDPI. Search combinations included "lithium-ion battery" with "state of health" or "SOH", together with "estimation", "diagnostics", "incremental capacity", "differential voltage", "impedance", "Kalman filter", "Gaussian process", "LSTM", "CNN", "Transformer", "physics-informed", "digital twin", "uncertainty", "cross-cell", "real-world", "battery passport", and "second life". Backward citation checking was used for foundational aging and diagnostic studies. No lower publication-date limit was imposed; the retained sources span 2005-2026.

Peer-reviewed English-language journal and conference papers were included when they addressed lithium-ion aging, SOH definition or estimation, validation, BMS implementation, sensing, or life-cycle decision making. Official regulatory documents and major institutional reports were included for policy claims. Studies concerned only with state of charge were retained only when they provided directly transferable observer, embedded-computing, or cross-chemistry evidence. Non-traceable numerical claims, duplicate records, and sources without a clear connection to SOH were excluded. After DOI-level deduplication and relevance screening, 117 unique publications, institutional reports, and regulatory documents formed the final evidence base. Because the review is structured narrative, exhaustive database hit counts and a PRISMA flow are not claimed.

1.2. Scope and Contribution Relative to Existing Reviews

Recent reviews provide strong foundations but differ in scope. Table 1 positions the present synthesis against representative reviews. Its specific contribution is to integrate aging mechanisms, estimator families, chemistry-dependent observability, validation hierarchy, uncertainty, embedded feasibility, regulation, and second-life decisions within one deployment-oriented framework.

Table 1. Scope comparison with representative SOH review literature

Review	Primary scope	Aging mechanisms	Advanced AI / hybrid	Validation / deployment	Regulation / second life
Ungurean et al. [13]	Models, methods, commercial devices	Limited	Pre-deep-learning emphasis	Commercial-device perspective	Limited
Sui et al. [14]	Non-probabilistic ML for SOH	Contextual	Machine learning	Data and generalization issues	Not primary
Oji et al. [15]	Data-driven SOH methods	Contextual	ML / deep learning	Critical analysis	Not primary
Su et al. [7]	Cell-to-pack SOH review	Included	Model, data, hybrid	Cell-to-pack perspective	Limited
Liu et al. [16]	Systematic review of deep learning	Contextual	CNN, sequence, hybrid	Deep-learning challenges	Not primary
Jiang et al. [17]	Battery-state estimation and BMS architectures	Included	On-board, cloud, integrated BMS	Architecture-focused	Limited
Present review	Deployment-oriented SOH synthesis	Integrated	Transformer, PINN, digital twin	Validation hierarchy, uncertainty, embedded BMS	Integrated

2. Factors Affecting Battery State of Health and Aging Mechanisms

The degradation of SOH in lithium-ion batteries is not an isolated process; rather, it is the result of asymmetric interactions between battery chemistry and operational stress factors. In the literature, the aging process is generally categorized into two main phenomena: calendar aging, which describes capacity losses occurring when the battery is not in active use, and cyclic aging, which encompasses deformations caused by continuous charge-discharge cycles. Storage temperature and state of charge (SOC) are the primary determinants governing the kinetics of calendar aging; specifically, an increase in the cell's electrochemical potential at high SOC accelerates the thermodynamic activation of side reactions. Cyclic aging, on the other hand, is based on the mechanical stresses and chemical degradation that occur during the physical migration of lithium ions between electrode lattice structures. These two types of aging occur simultaneously in the field, and it is critically important for SOH estimation algorithms to be able to decouple these intertwined non-linear dynamics [18-20].

2.1. Charge/Discharge Rate (C-rate) and Current Density

The C-rate values, which define the charging and discharging speeds, are direct determinants of the battery's mechanical integrity. Fast charging under high current densities creates a severe lithium concentration gradient between the outer surfaces and cores of the electrode particles, which induces volumetric stresses within the particle structure and leads to the formation of microscopic cracks (particle cracking). As illustrated in Figure 2, higher C-rates significantly increase the rate of capacity fade, thereby reducing the number of operational cycles available before reaching critical thresholds. The contact of these newly formed crack surfaces with the electrolyte initiates a continuous SEI formation cycle, making lithium loss chronic, while high current further complicates thermal aging processes by causing localized temperature increases through Joule heating [21, 22]. This relationship is evident from the divergence between the slow-charge (0.5C) and fast-charge (2C) trajectories in Figure 2, where rapid degradation from particle cracking and heating pushes the battery to the 80% EOL threshold much earlier in its service life. The two trajectories were drawn qualitatively from the experimental aging literature cited [21-24]; they are schematic and do not represent a universal quantitative aging law.

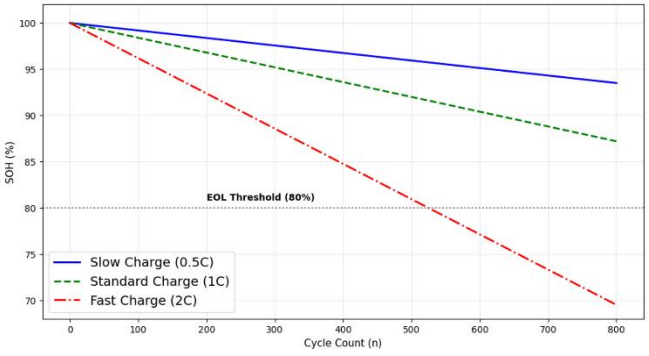


Figure 2. Conceptual influence of C-rate on degradation (authors' qualitative illustration, [21-24]).

2.2. Thermal Dynamics and the Impact of Temperature Gradients

Temperature is considered the dominant factor determining chemical reaction rates in the battery, in accordance with the Arrhenius law. However, the impact of temperature on SOH is not linear. At high temperatures (typically above 45°C), the SEI layer on the anode surface exhibits thermal instability; during the partial dissolution and reformation of this layer, active lithium ions are permanently consumed. This triggers the process defined as LLI, which is the primary driver of capacity loss; case studies on electric-vehicle packs report the same temperature-dominated ageing trend [25]. This temperature-driven degradation is clearly demonstrated in Figure 3, where the "Critical Zone," represented in deep red, expands significantly as ambient temperatures exceed 50°C. That heat

map was constructed qualitatively from the thermal and rate-dependent aging literature cited [8, 23, 24, 26]; its colour scale indicates relative degradation risk rather than measured or interpolated SOH values from a single dataset.

Conversely, low-temperature operations lead to increased electrolyte viscosity and reduced ionic diffusion, resulting in the "Lithium Plating" phenomenon. Ions that cannot enter the anode lattice during charging accumulate on the surface as metallic lithium, which not only reduces capacity but also fuels dendrite formations that pose a risk of puncturing the separator, thereby creating significant safety vulnerabilities [23, 24]. As evidenced by the SOH gradient in Figure 3, even moderate discharge rates become increasingly detrimental at extreme temperatures, demonstrating that the safest operational "Green Zone" is confined to a narrow window between 20°C and 30°C and only at low C-rates.

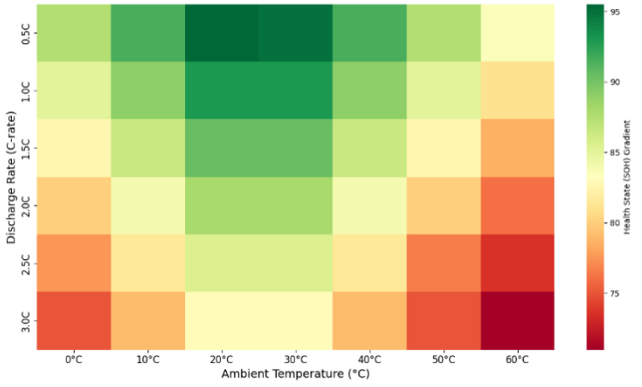


Figure 3. Qualitative interaction of temperature and C-rate in battery degradation (authors' conceptual heat map, [8, 23, 24, 26]).

2.3. Depth of Discharge (DOD) and Operational Range (SOC Windows)

The SOC range over which a battery is cycled plays a critical role in the rate of structural deformation; a battery continuously operated over a 0% to 100% SOC range (full DOD) undergoes more pronounced expansion and contraction of the cathode crystal lattice than during shallow cycling. These periodic volumetric changes lead to the structural collapse of the crystal lattice over time and the permanent loss of the capacity to host lithium ions (LAM), an effect that often leads industrial applications—particularly electric vehicle management software—to prefer shallow SOC windows and "software-protect" a portion of the battery capacity to extend its operational life [26, 27].

2.4. Dynamic Usage Profiles and Random Loading

In real-world applications, especially in electric vehicles, the dynamic usage profiles encountered diverge radically from the constant-current tests conducted in laboratory environments. Sudden high-current pulses occurring during regenerative braking and aggressive acceleration demands create transient dynamics by straining the ionic mobility within the battery. Such irregular loading prevents the establishment of chemical equilibrium within the battery, prolonging voltage relaxation times and rendering standard open-circuit voltage (OCV)-based estimations invalid. Furthermore, the nonuniform temperature distribution among cells in a battery pack causes some cells to age faster than others, creating a weakest-link effect. This situation necessitates not only cell-based but also system-level SOH management and advanced modeling techniques [28, 29].

2.5. Chemical and Environmental Side Reactions

Environmental factors and chemical interactions within the electrolyte constitute the invisible dimensions of the aging process. Depending on the sealing quality of the battery pack, any moisture that seeps in can react with lithium salts (LiPF6) in the electrolyte, leading to the formation of hydrofluoric acid (HF). This acidic environment accelerates capacity loss by corroding the electrode surfaces and increasing internal resistance. Furthermore, gas evolution resulting from electrolyte decomposition can increase internal cell pressure, potentially disrupting the contact between layers and raising ionic resistance, which negatively impacts the accuracy of SOH estimation. Consequently, an SOH estimation model must internalize not only electrical parameters but also the potential effects of chemical side reactions [30, 31].

2.6. Calendar Aging and Storage Stability

Calendar aging in lithium-ion batteries refers to the time-dependent degradation occurring under storage conditions without active cycling, driven by coupled electrochemical and thermodynamic processes [32]. The dominant degradation mechanism is associated with the progressive growth of the SEI layer on the anode surface. This growth is primarily induced by electrolyte reduction and solvent decomposition reactions, which irreversibly consume cyclable lithium inventory [33]. As a result, a gradual loss of capacity is observed, accompanied by an increase in internal resistance. These degradation pathways exhibit Arrhenius-type temperature dependence, where elevated temperatures significantly accelerate reaction kinetics and SEI thickening. Recent post-mortem studies have confirmed that these thermal stress factors are the primary cause of irreversible power fade in long-term stationary storage [34].

The kinetics of calendar aging are strongly influenced not only by temperature but also by SOC during storage. At high SOC levels, elevated cathode potential promote electrolyte oxidation and transition metal dissolution, further exacerbating degradation mechanisms [34]. However, even under low SOC conditions, prolonged storage leads to continuous SEI restructuring and lithium inventory loss. Recent studies emphasize that calendar aging cannot be treated independently from cycle aging in realistic operating scenarios, as both mechanisms are inherently coupled [35]. Consequently, advanced modeling approaches now integrate semi-empirical formulations with physics-based descriptions to bridge the gap

between laboratory storage tests and real-world battery life cycles, ensuring more accurate lifetime predictions.

2.7. Mechanical Vibration and Structural Integrity

Mechanical vibration is increasingly recognized as a critical external stress factor influencing lithium-ion battery aging, particularly in automotive, aerospace, and mobile applications. Recent studies demonstrate that vibration induces internal mechanical stresses within the cell structure, leading to electrode deformation, particle cracking, and loss of inter-particle contact [36]. These structural degradations accelerate key aging mechanisms such as LAM and LLI, ultimately resulting in increased internal resistance and capacity fade. For instance, experimental investigations reported that vibration exposure promotes electrode material detachment and enhances side reactions at electrode–electrolyte interfaces, thereby accelerating SEI growth and electrochemical degradation pathways. This mechanical fatigue often catalyzes chemical instability, creating a multi-physical aging environment.

Furthermore, vibration effects are not isolated but interact synergistically with other aging factors such as temperature and cycling conditions, leading to nonlinear degradation behavior. High-frequency or long-duration vibration can alter the internal stress distribution of the jelly-roll structure, exacerbating microstructural damage and reducing thermal stability [37]. Current literature suggests that neglecting vibration-induced stress can lead to a significant overestimation of SOH, especially in heavy-duty electric vehicle applications where road-induced frequencies are persistent. Consequently, incorporating vibration effects into lifetime prediction models and battery management strategies has become essential for accurate state-of-health estimation and robust system design.

3. SOH Estimation Methods

SOH estimation in lithium-ion batteries is one of the most complex and multidimensional tasks for BMSs. Since SOH is not a directly measurable physical quantity (unlike voltage or current), it is estimated indirectly by passing data from battery terminals through a filter comprising complex mathematical algorithms and physical models. The fundamental challenge in SOH estimation lies in the non-linear nature of battery aging and its asymmetric dependence on numerous external variables such as temperature, DOD, and the charge/discharge rate (C-rate). Approaches developed in the literature over the last thirty years are classified under four main paradigms based on computational cost, data requirements, accuracy, and real-time applicability criteria [38, 39]. The holistic taxonomy of these core paradigms is systematically illustrated in Figure 4, which is a conceptual synthesis of the method literature reviewed in Sections 3.1-3.4 [13-15, 39] rather than a bibliometric classification. In this section, the electrochemical foundations, algorithmic structures, and integration processes of these methods into industrial BMS architectures will be comprehensively analyzed in light of the most recent literature.

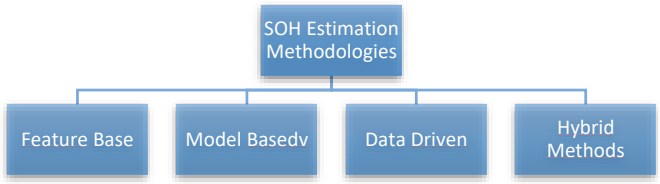


Figure 4. Taxonomy of battery SOH estimation methods (authors' conceptual synthesis, [13-15, 39]).

3.1. Feature-Based / Direct Measurement Methods

Feature-based methods rely on the analysis of specific parameters obtained from the battery's fundamental operating curves (voltage-time, current-voltage, etc.), which are referred to as "health indicators" (HIs) [40]. The core philosophy of these methods is to map complex electrochemical degradations occurring within the battery's internal structure to characteristic changes in externally observable signals. These approaches have become the most widely used methods in first-generation electric vehicles and portable systems because they do not require deeply intricate modeling of the battery's internal physics and possess a low computational burden [41].

3.1.1 Incremental Capacity Analysis (ICA) and Differential Applications

ICA is one of the most widely used analytical methods in battery characterization. This method makes the phase transitions within the battery visible by examining the relationship between voltage (V) and capacity (Q) data during charging or discharging in a differential form (dQ / dV) [42]. From a thermodynamic perspective, battery electrodes form specific potential plateaus during intercalation (insertion into the structure) or deintercalation of lithium ions. As the aging process progresses, the width and position of these plateaus shift. Mathematically, this analytical transformation computes the derivative of the capacity delivered or absorbed over a specific voltage interval, thereby converting voltage plateaus into clearly identifiable differential peaks:

$$IC(V) = \frac{dQ}{dV} = \frac{I * dt}{dV} \quad (3)$$

Eq. (3) defines incremental capacity IC(V) = dQ/dV = I(dt/dV), where Q is accumulated charge or capacity (Ah), V is terminal voltage (V), I is current (A), and t is time (h); IC therefore has units of Ah V^-1. The peaks on the ICA curve represent the phase transitions within the crystalline structure of the electrode material. For instance, as a Li-ion battery ages, the amplitude of these peaks decreases due to the LLI, while the points exhibit a shift along the voltage axis due to the LAM. In the literature, Dubarry et al. have developed methodologies that utilize the changes in the position and area of these peaks to determine which aging mechanism (anode or cathode) is more dominant [43, 44].

However, noise is the primary obstacle to the practical applications of ICA. The derivative computed from raw data amplifies even the smallest fluctuations in the signal, presenting them as large deviations. To overcome this problem, modern studies employ Savitzky-Golay (S-G) filters, Moving Average algorithms, or more advanced Gaussian Filtering techniques [45]. Particularly, recent studies in 2024 have focused on creating hybrid estimation architectures by feeding ICA curves as input into machine learning algorithms [46].

3.1.2 Differential Voltage Analysis (DVA) and Electrochemical Diagnostics

DVA is the mathematical inverse of ICA and evaluates dV/dQ as a function of capacity. Its principal value is the ability to track electrode-related transitions and changes in usable-capacity alignment through the voltage response [47, 48]. Peak position, amplitude, and shape may indicate changes in electrode balance or degradation mode, but interpretation depends on chemistry, temperature, current rate, smoothing, and the available capacity window.

$$DV(Q) = \frac{dV}{dQ} \tag{4}$$

Equation (4) defines differential voltage as dV/dQ, where V is terminal voltage (V) and Q is accumulated charge or discharge capacity (Ah); dV/dQ therefore has units of V Ah^-1. Because numerical differentiation amplifies noise, the sampling interval, filtering method, and charge/discharge rate should be reported. Incomplete or dynamic vehicle segments may not contain the electrode features required for reliable DVA, motivating reconstruction or probabilistic completion methods [49].

In contrast, the field application of DVA on vehicles faces significant constraints. In real-world driving conditions, batteries are rarely fully charged or discharged with a constant current (CC). Random current draws disrupt the stable data flow required to generate the DVA curve. Consequently, current research focuses on algorithms capable of performing DVA analysis over "partial charging segments" (e.g., using charging data only between 30%–50% SOC) and completing missing data through probabilistic methods [49].

3.1.3 Electrochemical Impedance Spectroscopy (EIS) and Frequency Domain Analysis

Internal resistance is the fastest and most prominent indicator of SOH change. However, the internal resistance of a battery is not a single resistance value (R); rather, it comprises multiple components with different time constants, such as ohmic resistance, charge-transfer resistance, and diffusion impedance. The EIS method measures the complex impedance response of the battery by applying a small-amplitude alternating current (AC) signal across a wide frequency band (typically between 10 mHz and 100 kHz) [50]. Mathematically, this sinusoidal excitation allows the system to evaluate the voltage-to-current ratio in the frequency domain, thereby capturing both the resistive and reactive behaviors of the cell layers:

$$Z(\omega) = \frac{V(\omega)}{I(\omega)} = \ R_{real} + \ j \ \cdot X_{img} \tag{5}$$

Here, Eq. (5) defines complex impedance Z(ω) = V(ω)/I(ω) = R_real + jX_img, where Z, R_real, and X_img are in ohms (Ω), V(ω) is the voltage phasor (V), I(ω) is the current phasor (A), ω is angular frequency (rad s^-1), and j is the dimensionless imaginary unit. The data obtained are represented on a Nyquist diagram (real impedance vs. imaginary impedance). The diameter of the semicircles in this diagram indicates the magnitude of the charge transfer resistance, a value that increases in direct proportion to the thickening of the SEI layer as the battery ages [51]. EIS is the most sensitive method for analyzing battery health at the "intracellular chemical level.

From an industrial perspective, the primary limitation of EIS is the cost and complexity of the hardware (potentiostat/galvanostat) required for these measurements. It is difficult for an on-board BMS to generate such precise AC signals. Consequently, "Fast Impedance Estimation" techniques have been developed in recent years [52]. In these techniques, researchers attempt to extract impedance information without disconnecting the battery system, using switching noise from the vehicle's electric motor drive (inverter) or specific current pulses.

3.1.4 Charge Curve Analysis and Time-Based Health Indicators

In practical BMS applications, the most widely used feature-based method tracks changes in time and voltage within specific regions of the charging curve. As the battery ages, the charging voltage rises more rapidly due to the increase in internal resistance, and the target voltage limit is reached much sooner [53]. This situation results in a reduction in the battery's charging time; however, this is not an increase in charging speed, but rather a symptom of capacity loss.

Researchers have defined the time required to traverse a specific voltage range (e.g., 3.7V - 4.1V) (Δt) or the amount of energy transferred to the battery within this voltage range (ΔE) as fundamental health indicators; these indicators generally exhibit linear or exponential relationships and are highly correlated with SOH. furthermore, since this approach requires only a timer and a voltmeter, it can operate successfully even on the lowest-cost BMS processors [54], although its accuracy is strictly dependent on temperature compensation because increased internal resistance in cold weather—independent of aging—could lead the system to erroneously label the battery as "aged."

3.2. Model-Based Estimation Methods

Model-based methods aim to estimate SOH by establishing a mathematical model of the battery's physical or electrical behavior and by changes in the model's parameters. Instead of treating the battery as a "black box," this approach simulates its internal dynamics using mathematical equations. Model-based approaches are fundamentally divided into two categories:

Equivalent Circuit Models (ECM) and Electrochemical Models (EM) [55].

3.2.1 Equivalent Circuit Models (ECMs) and Parameter Identification

Equivalent Circuit Models represent the electrochemical processes of the battery using fundamental electrical components such as resistors (R), capacitors (C), and voltage sources [56]. This method is optimal for real-time BMS applications because it requires significantly lower computational load than electrochemical models. The most commonly used structure is the Thevenin model, which comprises an ohmic resistor and one or more RC networks. Mathematically, the electrical behavior of this system is governed by a state-space formulation that links the transient voltage response across the RC networks to the overall cell terminal voltage:

$$V_t = OCV(SOC) - I * R_0 - V_{RC} \quad (6)$$

$$\frac{dV_{RC}}{dt} = -\frac{V_{RC}}{R_1 C_1} + \frac{I}{C_1} \quad (7)$$

Here, Eq. (6) defines terminal voltage V_t (V) from open-circuit voltage OCV(SOC) (V), current I (A), ohmic resistance R_0 (Ω), and RC polarization voltage V_RC (V). Equation (7) defines dV_RC/dt (V s^-1), where t is time (s), R_1 is polarization resistance (Ω), and C_1 is capacitance (F). R_0 and R_1 are key aging-sensitive parameters that generally increase as the battery ages. SOH estimation is performed through continuous online monitoring of these parameters. Algorithms such as Recursive Least Squares (RLS) or the Extended Kalman Filter (EKF) are generally employed for the instantaneous estimation of these parameters [57]. As aging progresses, the deviation of these resistance values from their initial values directly reflects the decline in the battery's power health (power fade) [5, 6].

3.2.2 Extended Kalman Filter (EKF) and Adaptive Approaches

Kalman filtering (KF) theory is considered the "gold standard" for battery state estimation (SOC and SOH) [58, 59]. However, since battery systems are highly non-linear, the standard KF proves insufficient. At this point, the EKF, which linearizes system equations using Taylor series expansion, comes into play.

EKF operates in a two-stage cycle: prediction and correction. For SOH estimation, the EKF is typically structured in "Dual" or "Joint" configurations. In the Dual-EKF architecture, the first filter estimates the SOC value (fast-changing state), while the second filter estimates capacity or resistance values (slow-changing parameters) associated with SOH [60]. This decoupling increases computational precision while maintaining the stability of the algorithm [61]. Mathematically, the state correction step in this filter leverages the discrepancy between the actual terminal voltage and the model's prediction to dynamically update the parameters:

$$\hat{x}_{(k|k)} = \hat{x}_{(k|k-1)} + K_k\left(z_k - h\left(\hat{x}_{(k|k-1)}\right)\right) \quad (8)$$

Equation (8) represents the EKF correction step. The estimated state vector x_hat (k|k) and prior estimate x_hat (k|k-1) have component-specific units defined by the selected state vector; k is the dimensionless discrete-time index. The measurement vector z_k and predicted measurement h(x_hat (k|k-1)) have the same measurement units (typically volts for terminal-voltage measurement), while K_k has state-unit per measurement-unit so that the correction term is dimensionally consistent. EKF performance depends on model structure, parameter identification, initialization, and process- and measurement-noise covariance selection [62].

3.2.3 Unscented Kalman Filter (UKF) and Sigma Points

The UKF, developed to eliminate the errors generated by the EKF during linearization (via Jacobian matrices), utilizes the "Sigma Points" technique, which directly models the probability distribution [63]. Instead of linearizing the battery's nonlinear structure, the UKF propagates that nonlinearity using sampling points.

UKF avoids explicit Jacobian linearization by propagating deterministically selected sigma points through the nonlinear model. Comparative studies show that EKF and UKF performance depends on model structure, parameterization, initialization, noise covariance, temperature, and operating profile; therefore, a universal percentage improvement or fixed computational-overhead ratio is not supported [63, 64]. UKF may improve robustness for strongly nonlinear conditions, but it requires more model evaluations per update and should be benchmarked on the target BMS hardware.

3.2.4 Particle Filters (PF) and Probabilistic Approaches

Battery aging is not only non-linear but is also subject to "non-Gaussian" noise (noise that does not follow a normal distribution). In such cases, Kalman-based filters reach their theoretical limits. PF methods model battery states by employing the Monte Carlo sampling method with a large number of "particles" (representative candidates) [65].

The greatest strength of PF in SOH estimation is its ability to merge remaining useful life (RUL) prediction and SOH estimation for the battery into a single framework. While the filter estimates the current capacity of the battery, it simultaneously presents the future decline trend of this capacity as a probability cloud [66]. This provides a confidence interval (95% CI) for when the battery pack will reach the "EOL" threshold.

3.2.5 Electrochemical Models (EM) and Physics-Based Observers

Unlike ECMs, electrochemical models are based on ion concentrations within the battery, diffusion coefficients, and kinetic processes defined by Butler-Volmer equations. The most

well-known model is the Doyle-Fuller-Newman (DFN) model [67]. This model can calculate SOH not merely in terms of an increase in resistance, but also in terms of nanometric changes in the thickness of the SEI layer or the loss of porosity in the active material. The following governing equation provides an analytical representation of this physical phenomenon, mapping the solid-phase transport of lithium species within the spherical electrode particles according to Fick's second law:

$$\frac{\partial c_s}{\partial t} = \frac{1}{r^2} * \frac{\partial}{\partial r}\left(D_s r^2 * \frac{\partial c_s}{\partial r} \right) \quad (9)$$

Equation (9) represents solid-phase diffusion, where c_s is solid-phase lithium concentration (mol m^-3), D_s is the solid diffusion coefficient (m^2 s^-1), r is radial position within an idealized active-material particle (m), and t is time (s). Physics-based models can improve interpretability and support degradation-mode analysis, but their fidelity depends on parameter identifiability, boundary conditions, thermal coupling, and model order. Full-order electrochemical models are generally too expensive for direct execution on a conventional BMS MCU; reduced-order or surrogate formulations are therefore used for real-time observers [67-69].

3.3. Data-Driven Estimation Methods

Data-driven methods are algorithmic structures that learn input-output relationships from large datasets (big data), rather than by directly modeling the battery's internal physics or electrochemical equations. These approaches can "learn" the multi-dimensional and non-linear nature of battery aging without requiring complex mathematical models. With the advancement of sensor technologies and the rise of cloud-based battery management systems, data-driven methods have become the most dominant research area in SOH estimation [14, 70]. Pack-level studies based on operational big data show that the same learning pipelines can be transferred from single cells to complete packs, provided that the label construction is stated explicitly [71].

3.3.1 Traditional Machine Learning: SVR and GPR Approaches

Before deep learning models became widespread, Support Vector Regression (SVR) and Gaussian Process Regression (GPR) formed the cornerstones of battery SOH estimation. SVR is an algorithm based on structural risk minimization and exhibits high generalization capability even in high-dimensional spaces. In SOH prediction, SVR is particularly known for preventing overfitting in small datasets [72, 73]. While these traditional frameworks provide solid theoretical baselines, modern automotive applications increasingly demand their deployment on production-grade silicon. For instance, leveraging the advanced diagnostic features of specialized chipsets like the L9963E BMS IC allows these machine learning models to operate efficiently at the edge, converting raw data into real-time state estimations [74].

Gaussian Process Regression (GPR) holds a unique place in SOH literature because it does not merely provide a prediction value, but also attaches an "uncertainty interval" (uncertainty quantification) to that prediction [75]. Using a Bayesian approach, GPR presents the SOH value as a probability distribution. From a formulation standpoint, this probabilistic regression framework is described by the following distribution equation:

$$f(x) \sim GP\big(m(x), k(x, x')\big) \quad (10)$$

Equation (10) denotes f(x) ~ GP(m(x), k(x, x')), where x and x' are input-feature vectors with component-specific units (or dimensionless after normalization), f(x) and m(x) have the units of the predicted target, and k(x, x') has squared target units. Kernel choice does not provide a universal percentage improvement; it encodes assumptions about smoothness and must be selected and validated for the available health indicators. A key advantage of Gaussian process regression is that it can provide a predictive distribution and calibrated uncertainty when its statistical assumptions are appropriate [75, 76].

3.3.2 Recurrent Neural Networks (RNN) and Long Short-Term Memory (LSTM)

Battery aging is inherently a time-series process. A battery's SOH today depends strongly on yesterday's operating conditions and its historical thermal profile. While standard Artificial Neural Networks (ANNs) cannot capture temporal dependencies between data points, Recurrent Neural Networks (RNNs) solve this problem through their memory mechanisms. However, standard RNNs suffer from the "vanishing gradient" problem during long-term dependencies [77].

LSTM networks use gating to represent temporal dependencies and can estimate SOH from charging sequences or engineered health indicators. For example, Liu et al. reported an RMSE below 1% for cases with the same discharge-current rate, but this is a study-specific result and does not establish equivalent performance for unseen cells, temperatures, chemistries, or field data [78]. Reporting should therefore include the split unit, operating domain, and whether test cells were absent from training.

$$f_t = \sigma\big(W_f \cdot [h_{t-1}, x_t] + b_f\big) \quad (11)$$

Equation (11) defines the dimensionless forget-gate vector f_t. The sigmoid activation σ is dimensionless; W_f is the forget-gate weight matrix, b_f is its bias vector, x_t is the input vector, h_(t-1) is the previous hidden-state vector, and t is the discrete-time index. With normalized neural-network inputs, these gating quantities are treated as dimensionless; with unnormalized physical inputs, W_f carries the reciprocal scaling required to keep the sigmoid argument dimensionless. Gated recurrent units use a simpler gating structure and can reduce parameter count, but on-board suitability must still be demonstrated through memory and execution-time measurements on the target processor [78].

3.3.3 Convolutional Neural Networks (CNN) and Image-Based SOH Diagnosis

CNNs, traditionally used for image processing, are utilized in battery literature to process voltage-current curves as "images" or "signatures" [79]. 1D-CNN models can automatically extract micro-changes (feature extraction) from charging curves. This capability spares researchers from the burden of manual feature engineering.

CNNs yield revolutionary results particularly when combined with transfer learning. For instance, a massive CNN model trained on laboratory data can be rapidly adapted to a new battery chemistry using a small amount of real-world data (fine-tuning) [80]. In a 2025 study, CNN-LSTM hybrid models—a combination of CNN and LSTM—have pushed SOH estimation precision to its peak by simultaneously extracting both instantaneous features (CNN) and temporal trends (LSTM) from the voltage curve [81].

3.3.4 Attention Mechanism and Transformer Architectures

Transformer and Attention mechanisms, which revolutionized the world of Natural Language Processing (NLP), have been recognized as the state-of-the-art technology in battery health estimation over the past two years [82]. Certain moments within battery data (e.g., periods of overheating or fast-charging intervals) have a much greater impact on aging than others. The attention mechanism enables the algorithm to focus on these critical moments.

Transformer architectures process sequence elements through attention and can capture long-range dependencies without recurrent state updates. Their comparative benefit depends on sequence length, feature construction, training-set size, and the baseline model; no universal stability improvement can be assigned to the architecture. Current battery studies report promising results but also identify data demand, computational cost, transferability, and interpretability as deployment barriers [82, 83].

3.4. Hybrid Methods and Physics-Informed Machine Learning

The most significant paradigm shift in SOH estimation literature over the past five years has been hybrid approaches that combine the precision of pure physical models with the flexibility of pure data-driven models [84]. Pure data-driven models (LSTM, CNN, etc.) can produce physically impossible results when exposed to extreme temperatures or to unexpected driving profiles that are not present in the training set (i.e., out-of-distribution). Hybrid methods aim to eliminate this problem by injecting "thermodynamic laws" and "electrochemical constraints" into artificial intelligence models [85-87].

3.4.1 Physics-Informed Neural Networks - PINN

PINN architecture is a groundbreaking approach in SOH estimation. While a standard neural network only tries to minimize the error (MSE) in input-output data, physical equations of the battery (e.g., Fick's law of diffusion or Butler-Volmer kinetics) are added to the loss function of PINNs as "penalty terms" [88]. The underlying dynamic behavior is represented by a composite objective function that ensures the network complies with both empirical observations and domain-specific conservation laws:

$$Loss = Loss_{data} + \lambda . Loss_{physics} \quad (12)$$

Equation (12) combines the data-fitting loss Loss_data and physics-based loss Loss_physics through the weighting coefficient λ. The loss terms are dimensionless when normalized residuals are used; λ is dimensionless in that case, otherwise it carries the scaling required to make the summed terms dimensionally compatible. The physical term can improve sample efficiency, extrapolation behavior, or consistency only when the selected physics and parameters are valid for the cell and operating domain. In a large study spanning 387 batteries and four datasets, Wang et al. reported a MAPE of 0.87%; this result is evidence for that specific framework and validation design, not a universal PINN advantage [84]. Other PINN formulations differ in which physics is encoded, ranging from a purely degradation-oriented residual [89] to a coupled electrochemical-thermal-mechanical constraint set [90], so their reported errors are not directly comparable with one another.

3.4.2 Model-Data Integration: EKF-ML Hybrid Structures

Another popular hybrid approach is the serial or parallel connection of a model-based observer, such as the EKF, with machine learning algorithms. In these structures, the EKF typically estimates parameters like the internal resistance and SOC of the battery in real-time, while a neural network (usually GRU or LSTM) compensates the system by predicting the EKF's modeling error (residual error) [91].

These "error-compensated" structures automatically correct deviations caused by changes in the physical parameters of the battery as it ages. For example, as the SEI layer inside the battery thickens, the fixed-parameter circuit model used by the EKF begins to produce erroneous results. The ML layer within the hybrid structure can learn residual model error and improve state-estimation robustness when the hybrid architecture is validated for the target cell and operating conditions [92, 93].

3.4.3 Digital Twin and Cloud-Based Hybrid Systems

With Industry 4.0, the concept of "Digital Twin" has become central to battery management. In this approach, a physical replica of each battery pack is maintained on cloud servers. While a simple model-based algorithm on-board the vehicle collects instantaneous data, massive "data-driven" models in the cloud perform in-depth analysis by comparing this data with historical data [94].

The Digital Twin architecture transforms SOH estimation from a mere detection of the current state into a "Fleet Learning" mechanism. Data coming from thousands of vehicles with similar driving profiles are used to train a single hybrid model

[95]. In this way, when a new vehicle hits the road, it begins SOH estimation with a hybrid model that already possesses thousands of kilometers of aging experience. Expanding this concept to entire vehicle fleets requires scalable algorithms capable of synchronized state tracking across multiple battery pack configurations without introducing massive computational overhead. Streamlined machine-learning frameworks have been investigated for state estimation in multi-pack electric-vehicle battery systems [96]. Digital-twin architectures with incremental learning have also been investigated for electric-vehicle battery management [97].

4. Comparative Analysis of SOH Estimation Methods and Application Challenges

The diversity of methodologies developed for SOH estimation of lithium-ion batteries stems from the fact that each method offers specific advantages and limitations tailored to a particular application scenario (e.g., electric vehicles, stationary energy storage systems, or portable electronics) [15]. The effectiveness of the methods presented in the literature should be evaluated through key metrics such as prediction accuracy, computational complexity, data dependency, and real-time feasibility [98]. This section presents a comprehensive comparison of the techniques detailed in Section 3 and discusses the fundamental bottlenecks encountered at the industrial scale. Earlier surveys have organized the same methods by algorithm family [99, 100]; the comparison below is instead organized by the evidence and the operating constraint that govern deployment.

4.1 Evaluation of Methods Based on Technical Metrics

Feature-based methods (ICA, DVA, EIS) are "transparent" models in that they provide direct evidence of the battery's internal physics. However, this transparency is balanced by the need for high-quality and noise-free data [98]. Given that differential approaches such as ICA and DVA are highly sensitive to sensor noise, their implementation in low-cost BMS hardware is challenging. These methods are generally preferred during laboratory battery characterization or the validation stages of new cell chemistries.

Model-based methods (EKF, UKF, PF) establish a reasonable balance between physical significance and real-time performance [101]. These filters, implemented using ECMs, can track battery dynamics while requiring low processing power. However, the accuracy of these models is strictly tied to the precision of initial parameters and the quality of the aging law. The greatest vulnerability of model-based approaches is that predictions can rapidly diverge when a scenario that is not included in the model (e.g., unexpected overheating or an accident) occurs.

Data-driven methods (LSTMs, CNNs, Transformers) eliminate the need to build complex physical models by generating solutions directly from raw data. The greatest strength of these methods lies in their ability to discover hidden aging patterns that cannot be perceived by the human eye or captured by simple models. However, these algorithms are characterized as "black-box" because they cannot provide a physical explanation for why a result was produced. Furthermore, they carry the risk of making significant errors when encountering battery chemistries or usage profiles not present in the training dataset (extrapolation) [39].

4.2 Representative Evidence and Context-Aware Comparison

Table 2 replaces generalized accuracy bands with representative, study-specific evidence. The reported results cannot be ranked as a universal league table because the studies differ in chemistry, cell count, signal window, SOH label, data split, and test domain. Their purpose is to demonstrate how performance should be reported and interpreted.

Table 2 demonstrates why algorithm-family accuracy ranges are misleading. A low error may reflect a narrow voltage segment, a within-domain test, or a favorable chemistry, whereas a higher field error may represent a more demanding and more transferable validation. Method selection should therefore prioritize the intended evidence level: laboratory diagnosis, embedded estimation on a known cell, cross-cell transfer, cross-temperature robustness, cross-chemistry transfer, or fleet-level field operation.

Data-driven and hybrid models should be evaluated for leakage between training and test cycles, repeated measurements from the same cell, hyperparameter selection on the test domain, and the absence of uncertainty calibration. Physics-informed constraints can improve consistency, but they do not replace external validation. A credible comparison reports the cell identity split, chemistry, temperature and duty-cycle range, partial-charge window, label construction, error metric, uncertainty method, and execution hardware.

4.3 Application Challenges and Bottlenecks in the Literature

Despite the theoretical laboratory successes of the methods, chronic problems encountered in real-world applications threaten the accuracy and reliability of SOH estimation. These challenges span a broad spectrum, from electrochemical complexity to hardware inadequacies.

4.3.1 Data Quality, Sensor Drift, and Electromagnetic Interference

Vehicle field data contain lower sampling rates, missing frames, sensor noise, cell imbalance, state-estimation error, and operating profiles that are absent from controlled laboratory cycling. These effects degrade differential features and capacity labels and can produce distribution shift for learned models [102, 103]. Liu et al.'s three-year dataset from 300 EVs illustrates that low-SOH samples and partial, noisy operating data remain more difficult than average test cases [102]. Filtering may improve signal quality, but its latency and computational cost must be reported rather than assuming a universal post-filter accuracy.

Table 2. Representative SOH estimation evidence with validation context

Method / study	Chemistry and data	Validation design	Reported result	Computation / uncertainty	Deployment interpretation
ICA / voltage-capacity model; He et al. [48]	Commercial Li-ion cells; constant-current laboratory charging data	Within-dataset validation on the authors' own cyclically aged cells	IC curve reconstructed from a voltage–capacity model instead of direct differentiation, reducing the noise amplification associated with raw dQ/dV and enabling SOH estimation from the reconstructed curve under the study's laboratory conditions	Low-to-moderate after smoothing; no native UQ	Physically interpretable; still requires an informative, low-noise charging segment, so the result is tied to that segment and to these cells
GP-ICE; Richardson et al. [76]	Oxford: 8 pouch cells; NASA: 20 cylindrical cells	Leave-one-cell-out; short galvanostatic segments	Best RMSPE 0.49% (Oxford) and 2.48% (NASA) for a 1450 s segment	GPR provides predictive uncertainty	Performance changes strongly with voltage window, duration, and dataset
EKF/UKF; Huang et al. [64]	Commercial Li-ion cell; first-order RC equivalent circuit and a combined model	Robustness comparison under unknown initial state, current noise, and temperature variation, for both models	UKF outperformed EKF in accuracy and convergence rate for both models, but the margin was distinctly smaller with the combined model; both filters were robust to current noise	Embedded-feasible; UKF requires more model evaluations	Confirms that the UKF advantage is model- and tuning-dependent, not a fixed improvement ratio; parameter adaptation is required on the target cell
LSTM-RNN; Liu et al. [78]	Charging-process health indicators	Controlled cases; same discharge-current-rate result reported	RMSE <1% in the stated same-rate cases	Training can be heavy; inference depends on model size; no native UQ	Do not extrapolate this number to unseen chemistry or field operation
PINN; Wang et al. [84]	387 batteries, 310,705 samples, four datasets	Regular, small-sample, and transfer experiments	MAPE 0.87% for the proposed framework	Physics regularization; training complexity remains	Strong multi-dataset evidence, but deployment hardware was not the primary endpoint
Multimodal field model; Liu et al. [102]	300 NCM EVs monitored for three years	Vehicle-level train/test evaluation on noisy partial-charge field data	Average MAPE 2.83%; MAPE 4.69% for SOH <85%	Cloud/GPU training; multimodal inputs; no simple on-board equivalence	Demonstrates the laboratory-to-field gap and low-SOH difficulty
EIS health indicators; Zhou et al. [51]	Li-ion cells; impedance spectra acquired under controlled measurement conditions	Study-specific laboratory validation across the cycling life of the tested cells	EIS-model parameters obtained directly by geometrically fitting two depressed semicircles in the intermediate-frequency range, which removes the iterative fitting step and greatly reduces identification cost	Requires excitation/measurement hardware; UQ method-dependent	High diagnostic value and a route towards online use, but on-board deployment still requires embedded excitation and impedance-measurement hardware

4.3.2 Chemical Variations and the "Flat Voltage" Problem

Battery chemistry changes the observability of health indicators. LFP cells exhibit a broad, relatively flat OCV-SOC region, so small voltage bias can cause large SOC or parameter uncertainty in that region; however, a universal conversion such as "1 mV equals 20% SOH error" is not physically valid without a specified OCV slope, temperature, aging state, and estimator [104, 105]. NMC voltage profiles often provide stronger slope information, but degradation-mode separation remains non-unique. Robust estimation therefore combines voltage with current, temperature, resistance or impedance, relaxation behavior, and history, and validates transfer explicitly for each chemistry. Unsupervised domain-adaptation results across chemistries indicate that a model transferred without target-domain adaptation degrades in a chemistry-dependent way

rather than uniformly [106]. Figure 5 illustrates this observability difference schematically; the curves are drawn from the chemistry-dependent estimation studies cited [102, 104-106] and are not taken from a common experimental dataset.

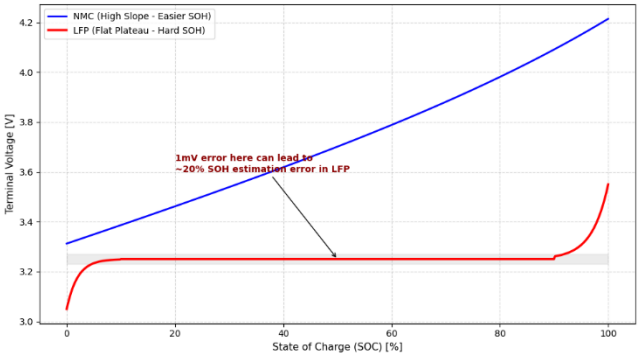


Figure 5. Schematic comparison of the voltage-profile observability of LFP and NMC chemistries (authors' qualitative illustration, [102, 104-106]).

4.3.3 Dynamic Usage Profiles and Capacity Regeneration (Recovery Effect)

In real-world use, batteries are not under a constant load as they are in laboratory tests. Long periods during which an automobile is parked or in low-current usage allow the ionic concentration within the battery to stabilize (relaxation). During this process, a phenomenon called "capacity regeneration" is observed; that is, when the battery rests for a while, its instantaneously measured capacity shows a slight increase [107, 108]. Static SOH models may perceive this physical recovery as the battery "rejuvenating" and produce unrealistic upward jumps in the SOH value. This situation leads to inconsistencies in the user's range estimation and faulty decision-making in the BMS safety protocols [107, 108]. Modeling this phenomenon requires a complex differential equation structure that takes into account not only the instantaneous state of the battery but also its "rest history"

4.3.4 Computational Cost, Memory Constraints and On-Board Feasibility

Large CNN and Transformer models may exceed the memory, latency, energy, and safety-assurance constraints of automotive microcontrollers. Feasibility must be demonstrated with parameter count, memory footprint, numerical precision, worst-case execution time, and target hardware [109, 110]. Model pruning, quantization, knowledge distillation, and edge-cloud partitioning can reduce cost, but they may change corner-case behavior and require revalidation [109, 111, 112].

4.4. Validation, Generalization, and Uncertainty

Validation claims should distinguish within-cell, cross-cycle, cross-cell, cross-temperature, cross-duty-cycle, cross-chemistry, external-dataset, and field validation. Randomly separating cycles from the same cell can leak cell-specific aging information into both training and test sets and generally provides weaker evidence than leaving complete cells or complete operating domains unseen. External validation should preserve the original model and preprocessing choices; otherwise, the exercise is adaptation rather than direct generalization.

Point accuracy alone is insufficient for safety- and value-critical decisions. Confidence intervals or predictive distributions should be checked for calibration, not merely reported. Gaussian-process, particle-filter, and other probabilistic data-driven approaches can represent predictive uncertainty, but the resulting interval or distribution must be evaluated for empirical coverage under the intended domain [65, 66, 75, 76, 113]. For field deployment, performance should also be stratified by SOH range, temperature, charge-window length, sensor quality, and chemistry.

4.5 Practical Method-Selection Guidance Across Operating Conditions

Sections 4.1-4.4 evaluate estimator families by technical metric, representative evidence, application challenge, and validation requirement. Table 3 consolidates this evidence into a decision-oriented view: for each recurring operating condition or constraint, it identifies the estimator family that is generally preferable, the reason, and the practical caveat that must still be managed. The guidance is directional rather than absolute, since the best choice for a given product still depends on the specific sensor set, chemistry, and validation evidence available.

No single estimator family is preferable across every row of Table 3: the binding constraint of the target application — chemistry, sensing quality, hardware budget, or the need for interpretability and calibrated uncertainty — should drive method selection, consistent with the deployment-oriented framework adopted throughout this review. This decision-oriented comparison, together with the validation hierarchy in Section 4.4, directly informs the BMS design guidance summarized in Section 6.

5. Future Perspectives: Limitations, Research Needs, and Technology Maturity

Future work should be driven by limitations demonstrated in Sections 4.3, 4.4, and 4.5. Near-term research should improve validation transparency, sensor-fault tolerance, uncertainty calibration, and compact embedded inference. Emerging directions include chemistry-aware transfer learning, multimodal field models, physics-informed learning, and edge-cloud digital twins. Longer-term concepts include validated in-cell sensing and autonomous health-aware control; these should be described as research directions rather than established capabilities. Figure 7 groups the functions discussed in this section by that maturity level; the grouping is a qualitative reading of the literature reviewed here and is not a quantified technology-readiness assessment.

Table 3. Practical method-selection guidance under representative operating conditions and constraints

Operating condition / constraint	Generally preferable method family	Rationale	Practical caveat
Partial charging / short voltage window	Equivalent-circuit model-based observers (EKF/UKF); short-segment feature indicators (e.g., GP-ICE) where available	ECM-based filters update online without a full charge/discharge cycle; short-segment feature methods can work, but reported error depends strongly on segment length and dataset [76]	Accuracy reported for a full cycle does not transfer to a shorter window; validate at the intended segment length
Dynamic current profiles (EV driving, regenerative braking)	Model-based filters (EKF/UKF/PF) with adapted parameters; data-driven models trained on matching duty cycles	Recursive filters track transient current integration; OCV-based feature methods assume relaxed equilibrium, which dynamic profiles disrupt [101]	Filter accuracy depends on correct parameter identification under load; data-driven models need training data containing the target duty cycle
High sensor noise / low-cost sensing	Probabilistic filters (EKF/UKF/PF) with explicit noise covariance	ICA/DVA differentiate the voltage curve, which amplifies noise; filters are designed to weight noisy measurements explicitly [98]	Filter performance depends on correctly specified noise covariance; misspecified covariance produces overconfident estimates
Wide temperature variation	Physics-informed or electrochemical model-based methods with temperature-dependent parameters	These can embed Arrhenius-type temperature dependence explicitly; models trained at one temperature range generalize poorly outside it [34]	Requires temperature as an explicit input and temperature-stratified validation, not only an aggregate error
LFP / flat-voltage, low-observability chemistries	Resistance- or impedance-based indicators, or multimodal/data-driven models; not voltage-slope features alone	A flat OCV-SOC region removes most voltage-based information; small voltage bias causes large uncertainty in that region [104, 105]	Even data-driven models need explicit validation in the low-slope region, not only an aggregate metric
Tight embedded compute / memory budget	Feature-based (ICA/DVA/EIS) or equivalent-circuit model-based methods; compressed data-driven models only if required	These have markedly lower online computational burden than large CNN/Transformer models [109-112]	Feasibility must be demonstrated on the target microcontroller, not assumed from a desktop benchmark
Physical interpretability required (warranty, certification, root-cause)	Feature-based or electrochemical model-based methods	These provide a traceable link to a physical quantity; pure data-driven models remain black-box [39]	Physics-informed hybrids restore interpretability only for the mechanisms they explicitly encode
Calibrated uncertainty required (safety-critical, second-life screening)	Probabilistic approaches such as Gaussian-process and particle-filter methods	These natively produce a distribution or interval rather than a point estimate [65, 66, 75, 76, 113]	The interval must be checked for empirical coverage in the target domain; an uncalibrated interval is as misleading as an unqualified point estimate
Limited or unlabeled field data	Feature-based or model-based methods that do not require large labeled datasets; physics-informed hybrids when some data exist	ICA/DVA/EIS and ECM-based filters operate without supervised aging labels, unlike purely data-driven models	Model-based methods still need accurate initial parameterization, which itself requires some characterization data

5.1 Smart Cells and In-Cell Sensor Technologies

Terminal voltage, current, and surface temperature provide only indirect information about internal gradients and mechanical change. Embedded fiber-optic and related in-cell optical sensing can add observability, but measurement accuracy, durability, calibration drift, manufacturability, cost, and safety must be demonstrated over cell life [114, 115]. These sensors do not provide "100% accuracy"; they provide additional signals that may reduce estimation uncertainty when fused with validated models.

The research need is therefore multimodal estimation with traceable calibration and fault detection. Potential solutions include sensor fusion, physics-constrained observers, self-diagnostics, and uncertainty-aware decision rules. Technology maturity varies: surface-temperature and terminal sensing are established; embedded fiber-optic sensing is emerging; fully autonomous smart cells with life-long self-calibration remain prospective.

5.2 New Battery Regulation (EU 2023/1542) and the Impact of Global Regulations

Regulation (EU) 2023/1542 establishes staged requirements for battery information, durability, state-of-health-related data, due diligence, recycled content, recycling efficiency, material recovery, and the battery passport. The legal text should be cited directly because implementation dates and scope vary by battery category [12]. SOH algorithms support compliance and life-cycle decisions, but the Regulation does not make a single estimator or universal second-life SOH threshold legally mandatory.

Figure 6 presents an engineering decision sequence rather than a legal decision rule. The displayed 80% and 60% SOH points are illustrative thresholds frequently used in discussions of first-life retirement and second-life screening; they are not universal limits imposed by Regulation (EU) 2023/1542. Actual routing to continued use, repurposing, remanufacturing, or recycling requires application-specific performance and safety assessment together with the applicable regulatory obligations [11, 12].

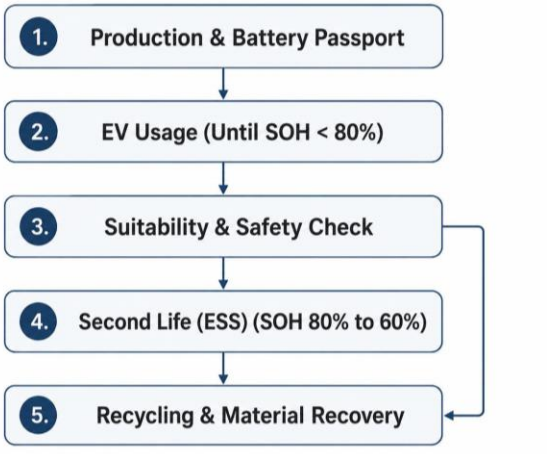


Figure 6. Conceptual circular-economy decision framework (authors' illustration, [11, 12])

5.2.1 Mandatory Access to SOH and SOC Data

Regulatory access to battery information increases the importance of transparent definitions, traceable calibration, software versioning, and auditable uncertainty. A reported SOH value should identify whether it is capacity-, resistance-, or power-based and should retain the conditions and data history needed to interpret it. Independent access does not, by itself, make different manufacturers' SOH values comparable.

5.2.2 Battery Passport and Carbon Footprint

From 18 February 2027, Regulation (EU) 2023/1542 requires a battery passport for specified categories, including EV batteries and industrial batteries above the stated capacity threshold. The passport is a data-access framework; the applicable content, access rights, and implementation details should be read from the Regulation and delegated acts rather than inferred from a conceptual figure [12].

5.2.3 Second Life and Recycling Targets

Second-life suitability cannot be decided from SOH alone. Screening should combine capacity and power capability with insulation, fault history, thermal exposure, cell imbalance, mechanical integrity, and the duty of the destination system. Technical screening is also inseparable from the legal and economic conditions of the destination application, which differ by jurisdiction and by ownership model [116]. Regulation (EU) 2023/1542 also sets staged recycling-efficiency and material-recovery targets; the exact target, material, date, and denominator must be quoted directly when used [11, 12].

5.2.4 Global Standards: Euro 7 and Chinese Regulations

Euro 7 introduces staged traction-battery durability requirements for light- and heavy-duty vehicles. These requirements should not be paraphrased as a single universal warranty threshold because the applicable retained-energy values depend on vehicle category, time, and mileage. International data-reporting and durability rules also differ in scope and measurement definition; cross-jurisdictional comparison therefore requires the original legal or standards document [117].

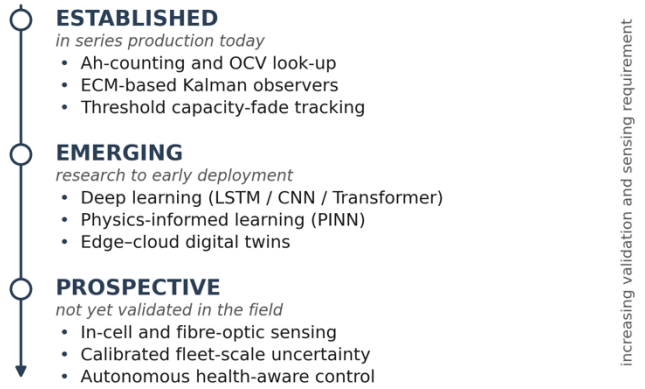


Figure 7. Technology-maturity map of SOH estimation and battery-management functions (authors' conceptual synthesis, [84, 93, 96, 110, 114, 115])

6. Conclusions

This structured narrative review shows that SOH estimation is an evidence-selection problem as much as an algorithm-selection problem. Capacity-, resistance-, and power-based definitions are not interchangeable, and reported errors cannot be compared without chemistry, operating conditions, SOH labels, validation splits, and metrics.

Feature-based methods provide interpretable degradation indicators but require informative and sufficiently clean signal segments. Equivalent-circuit observers remain attractive for embedded use, although parameter drift and model mismatch require adaptation. Data-driven methods can model nonlinear aging from partial data, but low within-domain error does not demonstrate cross-cell, cross-temperature, cross-chemistry, or field robustness. Physics-informed and hybrid methods are promising when the added constraints are valid and their computational and validation costs are reported.

No method family is universally superior. A defensible BMS design should match the estimator to the available sensors, chemistry, duty cycle, hardware, required update rate, and decision risk (Table 3). It should also quantify uncertainty,

monitor sensor and model drift, and retain a fallback strategy for operation outside the validated domain.

The most important research priorities are transparent validation hierarchies, external and field datasets, chemistry-aware transfer, calibrated uncertainty, compact edge implementation, and multimodal sensing with life-long calibration. Regulatory and second-life decisions will additionally require auditable SOH definitions and traceable battery histories. Progress should therefore be measured not only by lower laboratory error, but by reproducible performance under unseen and safety-relevant conditions.

Conflict of Interest Statement

The authors declare that there is no conflict of interest in the study.

CRediT Author Statement

Hakan Çoban: Conceptualization, Visualization, Writing-original draft, Investigation, Methodology, Resources
Mustafa Baysal: Conceptualization, Supervision, Writing – Review & Editing, Project Administration
Koray Erhan: Investigation, Methodology, Supervision, Writing – Review & Editing, Resources

Declaration of Generative AI in the Writing Process

During the preparation of this manuscript, the authors used Microsoft 365 Copilot for language editing and proofreading purposes (e.g., grammar, spelling, punctuation, and clarity improvements) and to assist in improving the readability of the text. All AI-assisted output was subsequently reviewed and, where necessary, edited by the authors, who take full responsibility for the final content of the manuscript.

References

[1] Armand M, Tarascon JM. Building better batteries. Nature. 2008;451(7179):652–657. https://doi.org/10.1038/451652a

[2] Goodenough JB, Park KS. The Li-ion rechargeable battery: A perspective. J Am Chem Soc. 2013;135(4):1167–1176. https://doi.org/10.1021/ja3091438

[3] International Energy Agency. Global EV Outlook 2024. Paris: IEA; 2024. https://www.iea.org/reports/global-ev-outlook-2024

[4] Solmaz H, Kocakulak T. Determination of Lithium Ion Battery Characteristics for Hybrid Vehicle Models. Int J Automot Sci Technol. 2020;4(4):264–271. https://doi.org/10.30939/ijastech..723043

[5] Vetter J, Novák P, Wagner MR, Veit C, Möller KC, Besenhard JO, et al. Ageing mechanisms in lithium-ion batteries. J Power Sources. 2005;147(1–2):269–281. https://doi.org/10.1016/j.jpowsour.2005.01.006

[6] Hu X, Xu L, Lin X, Pecht M. Battery Lifetime Prognostics. Joule. 2020;4(2):310–346. https://doi.org/10.1016/j.joule.2019.11.018

[7] Su L, Xu Y, Dong Z. State‐of‐health estimation of lithium‐ion batteries: A comprehensive literature review from cell to pack levels. Energy Convers Econ. 2024;5(4):224 – 242. https://doi.org/10.1049/enc2.12125

[8] Dubarry M, Truchot C, Liaw BY. Synthesize battery degradation modes via a diagnostic and prognostic model. J Power Sources. 2012;219:204–216. https://doi.org/10.1016/j.jpowsour.2012.07.016

[9] Bruj O, Calborean A. Electrochemical Impedance Spectroscopy Investigation on the Charge–Discharge Cycle Life Performance of Lithium-Ion Batteries. Energies. 2025;18(6):1324. https://doi.org/10.3390/en18061324

[10] Wahab A, Cifterler N, Amjady N, Date A, Kemper H, Khayyam H. Enhancing energy and thermal efficiency of single-phase liquid immersion cooling systems for lithium-ion batteries in electric vehicles. J Energy Storage. 2025;131:117365. https://doi.org/10.1016/j.est.2025.117365

[11] Iqbal H, Sarwar S, Kirli D, Shek JKH, Kiprakis AE. A survey of second-life batteries based on techno-economic perspective and applications-based analysis. Carbon Neutrality. 2023;2(1):8. https://doi.org/10.1007/s43979-023-00049-5

[12] European Parliament and Council of the European Union. Regulation (EU) 2023/1542 of the European Parliament and of the Council of 12 July 2023 concerning batteries and waste batteries, amending Directive 2008/98/EC and Regulation (EU) 2019/1020 and repealing Directive 2006/66/EC. Off J Eur Union. 2023;L191:1–117. https://eur-lex.europa.eu/eli/reg/2023/1542/oj

[13] Ungurean L, Cârstoiu G, Micea MV, Groza V. Battery state of health estimation: a structured review of models, methods and commercial devices. Int J Energy Res. 2017;41(2):151–181. https://doi.org/10.1002/er.3598

[14] Sui X, He S, Vilsen SB, Meng J, Teodorescu R, Stroe DI. A review of non-probabilistic machine learning-based state of health estimation techniques for Lithium-ion battery. Appl Energy. 2021;300:117346. https://doi.org/10.1016/j.apenergy.2021.117346

[15] Oji T, Zhou Y, Ci S, Kang F, Chen X, Liu X. Data-Driven Methods for Battery SOH Estimation: Survey and a Critical Analysis. IEEE Access. 2021;9:126903–126916. https://doi.org/10.1109/access.2021.3111927

[16] Liu C, Li H, Li K, Wu Y, Lv B. Deep Learning for State of Health Estimation of Lithium-Ion Batteries in Electric Vehicles: A Systematic Review. Energies. 2025;18(6):1463. https://doi.org/10.3390/en18061463

[17] Jiang M, Li D, Li Z, Chen Z, Yan Q, Lin F, et al. Advances in battery state estimation of battery management system in electric vehicles. J Power Sources. 2024;612:234781. https://doi.org/10.1016/j.jpowsour.2024.234781

[18] Li R, Kirkaldy ND, Oehler FF, Marinescu M, Offer GJ, O'Kane SEJ. The importance of degradation mode analysis in parameterising lifetime prediction models of lithium-ion battery degradation. Nat Commun. 2025;16(1):2776. https://doi.org/10.1038/s41467-025-57968-3

[19] Wildfeuer L, Karger A, Aygül D, Wassiliadis N, Jossen A, Lienkamp M. Experimental degradation study of a commercial

lithium-ion battery. J Power Sources. 2023;560:232498. https://doi.org/10.1016/j.jpowsour.2022.232498

[20] Raj T, Wang AA, Monroe CW, Howey DA. Investigation of Path‐Dependent Degradation in Lithium‐Ion Batteries¥*¥*. Batteries Supercaps. 2020;3(12):1377 – 1385. https://doi.org/10.1002/batt.202000160

[21] Qu JG, Jiang ZY, Zhang JF. Investigation on lithium-ion battery degradation induced by combined effect of current rate and operating temperature during fast charging. J Energy Storage. 2022;52:104811. https://doi.org/10.1016/j.est.2022.104811

[22] Xie W, He R, Gao X, Li X, Wang H, Liu X, et al. Degradation identification of LiNi0.8Co0.1Mn0.1O2/graphite lithium-ion batteries under fast charging conditions. Electrochim Acta. 2021;392:138979. https://doi.org/10.1016/j.electacta.2021.138979

[23] Peng Y, Zhong C, Ding M, Zhang H, Jin Y, Hu Y, et al. Quantitative Analysis of Active Lithium Loss and Degradation Mechanism in Temperature Accelerated Aging Process of Lithium‐Ion Batteries. Adv Funct Mater. 2024;34(42):2404495. https://doi.org/10.1002/adfm.202404495

[24] Wu W, Ma R, Liu J, Liu M, Wang W, Wang Q. Impact of low temperature and charge profile on the aging of lithium-ion battery: Non-invasive and post-mortem analysis. Int J Heat Mass Transf. 2021;170:121024. https://doi.org/10.1016/j.ijheatmasstransfer.2021.121024

[25] Serarslan B. A review and case study about the impact of temperature and ageing on electric vehicle batteries. Int J Automot Eng Technol. 2025;14(4):229–244. https://doi.org/10.18245/ijaet.1519648

[26] Gao Y, Jiang J, Zhang C, Zhang W, Jiang Y. Aging mechanisms under different state-of-charge ranges and the multi-indicators system of state-of-health for lithium-ion battery with Li(NiMnCo)O2 cathode. J Power Sources. 2018;400:641–651. https://doi.org/10.1016/j.jpowsour.2018.07.018

[27] Zhu J, Xu W, Knapp M, Dewi Darma MS, Mereacre L, Su P, et al. A method to prolong lithium-ion battery life during the full life cycle. Cell Rep Phys Sci. 2023;4(7):101464. https://doi.org/10.1016/j.xcrp.2023.101464

[28] Li Y, Liu K, Foley AM, Zülke A, Berecibar M, Nanini-Maury E, et al. Data-driven health estimation and lifetime prediction of lithium-ion batteries: A review. Renew Sustain Energy Rev. 2019;113:109254. https://doi.org/10.1016/j.rser.2019.109254

[29] Keil P, Jossen A. Impact of Dynamic Driving Loads and Regenerative Braking on the Aging of Lithium-Ion Batteries in Electric Vehicles. J Electrochem Soc. 2017;164(13):A3081–A3092. https://doi.org/10.1149/2.0801713jes

[30] Liao Y, Zhang H, Peng Y, Hu Y, Liang J, Gong Z, et al. Electrolyte Degradation During Aging Process of Lithium‐Ion Batteries: Mechanisms, Characterization, and Quantitative Analysis. Adv Energy Mater. 2024;14(18):2304295. https://doi.org/10.1002/aenm.202304295

[31] Vennam G, Sahoo A, Ahmed S. A survey on lithium-ion battery internal and external degradation modeling and state of health estimation. J Energy Storage. 2022;52:104720. https://doi.org/10.1016/j.est.2022.104720

[32] Keil P, Schuster SF, Wilhelm J, Travi J, Hauser A, Karl RC, et al. Calendar Aging of Lithium-Ion Batteries. J Electrochem Soc. 2016;163(9):A1872–A1880. https://doi.org/10.1149/2.0411609jes

[33] Zhu W, Zhou P, Ren D, Yang M, Rui X, Jin C, et al. A mechanistic calendar aging model of lithium‐ion battery considering solid electrolyte interface growth. Int J Energy Res. 2022;46(11):15521–15534. https://doi.org/10.1002/er.8249

[34] Sordi G, Luder D, Li W, Sauer DU, Casalegno A, Rabissi C. Investigation of calendar ageing of lithium-ion battery through physical models with ex-situ validation. J Power Sources. 2024;615:235076. https://doi.org/10.1016/j.jpowsour.2024.235076

[35] Karger A, O'Kane SEJ, Rogge M, Kirst C, Singer JP, Marinescu M, et al. Modeling Particle Versus SEI Cracking in Lithium-Ion Battery Degradation: Why Calendar and Cycle Aging Cannot Simply be Added. J Electrochem Soc. 2024;171(9):090512. https://doi.org/10.1149/1945-7111/ad76da

[36] Awan U, Ghabraie K, Zolfagharian A, Rolfe B. Impact of vibrations on lithium-ion batteries in electric vehicles: sources, degradation mechanisms, and testing standards. J Phys Energy. 2025;7(2):022003. https://doi.org/10.1088/2515-7655/adb5c0

[37] Aravind Reddy B. An Overview of the Impact of Vibrations on Li‐Ion Battery Performance, Degradation, Battery Thermal Management System and Key Focus Areas. Eng Rep. 2025;7(6):e70235. https://doi.org/10.1002/eng2.70235

[38] Csikós F, Csikós F. Testing the Real Capacity of the Battery. Engineering Perspective. 2025;5(1st Future of Vehicles Conf.):1–7. https://doi.org/10.64808/engineeringperspective.1791078

[39] How DNT, Hannan MA, Hossain Lipu MS, Ker PJ. State of Charge Estimation for Lithium-Ion Batteries Using Model-Based and Data-Driven Methods: A Review. IEEE Access. 2019;7:136116–136136. https://doi.org/10.1109/access.2019.2942213

[40] Bian X, Wei ZG, Li W, Pou J, Sauer DU, Liu L. State-of-Health Estimation of Lithium-ion Batteries by Fusing an Open-Circuit-Voltage Model and Incremental Capacity Analysis. IEEE Trans Power Electron. 2022;37(2):2226–2236. https://doi.org/10.1109/TPEL.2021.3104723

[41] Gismero A, Nørregaard K, Johnsen B, Stenhøj L, Stroe DI, Schaltz E. Electric vehicle battery state of health estimation using Incremental Capacity Analysis. J Energy Storage. 2023;64:107110. https://doi.org/10.1016/j.est.2023.107110

[42] Sarıkurt T, Ceylan M, Balıkçı A. A parametric battery state of health estimation method for electric vehicle applications. Turk J Electr Eng Comput Sci. 2017;25(4):2860–2870. https://doi.org/10.3906/elk-1602-118

[43] Dubarry M, Anseán D. Best practices for incremental capacity analysis. Front Energy Res. 2022;10:1023555. https://doi.org/10.3389/fenrg.2022.1023555

[44] Ansean D, Garcia VM, Gonzalez M, Blanco-Viejo C, Viera JC, Pulido YF, et al. Lithium-Ion Battery Degradation Indicators Via

Incremental Capacity Analysis. IEEE Trans Ind Appl. 2019;55(3):2992–3002. https://doi.org/10.1109/tia.2019.2891213

[45] Peng HF, Huang GM. Noisy blind source separation based on CEEMD and Savitzky-Golay filter. IOP Conf Ser Mater Sci Eng. 2017;231:012185. https://doi.org/10.1088/1757-899x/231/1/012185

[46] Xu Z, Chen Z, Yang L, Zhang S. State of health estimation for lithium-ion batteries based on incremental capacity analysis and Transformer modeling. Appl Soft Comput. 2024;165:112072. https://doi.org/10.1016/j.asoc.2024.112072

[47] Olson JZ, López CM, Dickinson EJF. Differential Analysis of Galvanostatic Cycle Data from Li-Ion Batteries: Interpretative Insights and Graphical Heuristics. Chem Mater. 2023;35(4):1487–1513. https://doi.org/10.1021/acs.chemmater.2c01976

[48] He J, Wei Z, Bian X, Yan F. State-of-Health Estimation of Lithium-Ion Batteries Using Incremental Capacity Analysis Based on Voltage–Capacity Model. IEEE Trans Transp Electrif. 2020;6(2):417–426. https://doi.org/10.1109/tte.2020.2994543

[49] Bilfinger P, Rosner P, Schreiber M, Kröger T, Gamra KA, Ank M, et al. Battery pack diagnostics for electric vehicles: Transfer of differential voltage and incremental capacity analysis from cell to vehicle level. eTransportation. 2024;22:100356. https://doi.org/10.1016/j.etran.2024.100356

[50] Liu Y, Wang L, Li D, Wang K. State-of-health estimation of lithium-ion batteries based on electrochemical impedance spectroscopy: a review. Prot Control Mod Power Syst. 2023;8(1):41. https://doi.org/10.1186/s41601-023-00314-w

[51] Zhou Z, Li Y, Wang QG, Yu J. Health Indicators Identification of Lithium-Ion Battery From Electrochemical Impedance Spectroscopy Using Geometric Analysis. IEEE Trans Instrum Meas. 2023;72:1–9. https://doi.org/10.1109/tim.2023.3272401

[52] Sihvo J, Stroe DI, Messo T, Roinila T. Fast Approach for Battery Impedance Identification Using Pseudo-Random Sequence Signals. IEEE Transactions on Power Electronics. 2020;35(3):2548–2557. https://doi.org/10.1109/tpel.2019.2924286

[53] Xiong R, Zhang Y, Wang J, He H, Peng S, Pecht M. Lithium-Ion Battery Health Prognosis Based on a Real Battery Management System Used in Electric Vehicles. IEEE Trans Veh Technol. 2019;68(5):4110–4121. https://doi.org/10.1109/tvt.2018.2864688

[54] Ang EYM, Paw YC. Linear Model for Online State of Health Estimation of Lithium-Ion Batteries Using Segmented Discharge Profiles. IEEE Trans Transp Electrif. 2023;9(2):2464–2471. https://doi.org/10.1109/tte.2022.3206469

[55] Vasta E, Scimone T, Nobile G, Eberhardt O, Dugo D, De Benedetti MM, et al. Models for Battery Health Assessment: A Comparative Evaluation. Energies. 2023;16(2):632. https://doi.org/10.3390/en16020632

[56] Li F, Li Z, Zhang Y, Xu G, Wang X, Zhang H. Analysis and Verification of Equivalent Circuit Model of Soft-Pack Lithium Batteries. Energies. 2025;18(3):510. https://doi.org/10.3390/en18030510

[57] Naseri F, Schaltz E, Stroe DI, Gismero A, Farjah E. An Enhanced Equivalent Circuit Model With Real-Time Parameter Identification for Battery State-of-Charge Estimation. IEEE Trans Ind Electron. 2022;69(4):3743–3751. https://doi.org/10.1109/tie.2021.3071679

[58] He Z, Yang Z, Cui X, Li E. A Method of State-of-Charge Estimation for EV Power Lithium-Ion Battery Using a Novel Adaptive Extended Kalman Filter. IEEE Trans Veh Technol. 2020;69(12):14618–14630. https://doi.org/10.1109/tvt.2020.3032201

[59] Xu W, Wang S, Jiang C, Fernandez C, Yu C, Fan Y, et al. A novel adaptive dual extended Kalman filtering algorithm for the Li‐ion battery state of charge and state of health co‐estimation. Int J Energy Res. 2021;45(10):14592–14602. https://doi.org/10.1002/er.6719

[60] Beelen H, Bergveld HJ, Donkers MCF. Joint Estimation of Battery Parameters and State of Charge Using an Extended Kalman Filter: A Single-Parameter Tuning Approach. IEEE Trans Control Syst Technol. 2021;29(3):1087–1101. https://doi.org/10.1109/tcst.2020.2992523

[61] Jiang S, Shi J, Borah M, Moura S. Weaknesses and Improvements of the Extended Kalman Filter for Battery State-of-Charge and State-of-Health Estimation. In: 2024 American Control Conference (ACC); 2024. p. 1441–1448. https://doi.org/10.23919/acc60939.2024.10644628

[62] Xiong R, He H, Sun F, Zhao K. Evaluation on State of Charge Estimation of Batteries With Adaptive Extended Kalman Filter by Experiment Approach. IEEE Trans Veh Technol. 2013;62(1):108–117. https://doi.org/10.1109/tvt.2012.2222684

[63] He W, Williard N, Chen C, Pecht M. State of charge estimation for electric vehicle batteries using unscented kalman filtering. Microelectron Reliab. 2013;53(6):840–847. https://doi.org/10.1016/j.microrel.2012.11.010

[64] Huang C, Wang Z, Zhao Z, Wang L, Lai CS, Wang D. Robustness Evaluation of Extended and Unscented Kalman Filter for Battery State of Charge Estimation. IEEE Access. 2018;6:27617–27628. https://doi.org/10.1109/access.2018.2833858

[65] Li X, Yuan C, Wang Z, He J, Yu S. Lithium battery state-of-health estimation and remaining useful lifetime prediction based on non-parametric aging model and particle filter algorithm. eTransportation. 2022;11:100156. https://doi.org/10.1016/j.etran.2022.100156

[66] Dong G, Chen Z, Wei J, Ling Q. Battery Health Prognosis Using Brownian Motion Modeling and Particle Filtering. IEEE Trans Ind Electron. 2018;65(11):8646–8655. https://doi.org/10.1109/tie.2018.2813964

[67] Brosa Planella F, Ai W, Boyce AM, Ghosh A, Korotkin I, Sahu S, et al. A continuum of physics-based lithium-ion battery models reviewed. Prog Energy. 2022;4(4):042003. https://doi.org/10.1088/2516-1083/ac7d31

[68] Li J, Adewuyi K, Lotfi N, Landers RG, Park J. A single particle model with chemical/mechanical degradation physics for lithium ion battery State of Health (SOH) estimation. Appl Energy. 2018;212:1178–1190. https://doi.org/10.1016/j.apenergy.2018.01.011

[69] He W, Han T, Song H, Wang Q, Kang J, Wang JV, et al. An extended single-particle model of lithium-ion batteries based on simplified

solid-liquid diffusion process. iScience. 2024;27(11):110764. https://doi.org/10.1016/j.isci.2024.110764

[70] Roman D, Saxena S, Robu V, Pecht M, Flynn D. Machine learning pipeline for battery state-of-health estimation. Nat Mach Intell. 2021;3(5):447–456. https://doi.org/10.1038/s42256-021-00312-3

[71] Song L, Zhang K, Liang T, Han X, Zhang Y. Intelligent state of health estimation for lithium-ion battery pack based on big data analysis. J Energy Storage. 2020;32:101836. https://doi.org/10.1016/j.est.2020.101836

[72] Qian L, Xuan L, Chen J. Battery SOH estimation based on decision tree and improved support vector machine regression algorithm. Front Energy Res. 2023;11:1218580. https://doi.org/10.3389/fenrg.2023.1218580

[73] Dikmen IC, Yildiran N, Karadag T. Machine Learning Approaches for Enhancing the SoH Estimation of LTO Batteries. Int J Automot Sci Technol. 2025;9(1):48–59. https://doi.org/10.30939/ijastech..1522403

[74] Mühendis A, Akkaya R. Integrating Machine Learning with Advanced Features of L9963E BMS for Enhanced State of Charge Estimation. Int J Automot Sci Technol. 2025;9(4):475–490. https://doi.org/10.30939/ijastech..1698286

[75] Richardson RR, Osborne MA, Howey DA. Gaussian process regression for forecasting battery state of health. J Power Sources. 2017;357:209–219. https://doi.org/10.1016/j.jpowsour.2017.05.004

[76] Richardson RR, Birkl CR, Osborne MA, Howey DA. Gaussian Process Regression for In Situ Capacity Estimation of Lithium-Ion Batteries. IEEE Trans Ind Inform. 2019;15(1):127–138. https://doi.org/10.1109/tii.2018.2794997

[77] Wang C, Bao Z, Lin H, Nie J, Zhu C. A Multitask Targeted Learning Framework for Lithium-Ion Battery State-of-Health and Remaining Useful Life. IEEE Trans Transp Electrif. 2026;12(1):32–44. https://doi.org/10.1109/tte.2025.3610457

[78] Liu K, Kang L, Xie D. Online State of Health Estimation of Lithium-Ion Batteries Based on Charging Process and Long Short-Term Memory Recurrent Neural Network. Batteries. 2023;9(2):94. https://doi.org/10.3390/batteries9020094

[79] Costa N, Sánchez L, Anseán D, Dubarry M. Li-ion battery degradation modes diagnosis via Convolutional Neural Networks. J Energy Storage. 2022;55:105558. https://doi.org/10.1016/j.est.2022.105558

[80] Lin M, Ke L, Meng J, Wu J, Stroe DI. An Ensemble Convolutional Neural Network Based Transfer Learning Framework for Achievable Lithium-Ion Battery Health Perception in Flexible Charging Procedure. IEEE ASME Trans Mechatron. 2025;30(6):5420–5431. https://doi.org/10.1109/tmech.2025.3561027

[81] Xiao F, Yang W, Ding Y, Li X, Zhang K, Liu J. A CNN‐LSTM Method Based on Voltage Deviation for Predicting the State of Health of Lithium‐Ion Batteries. Battery Energy. 2025;4(3):e20240036. https://doi.org/10.1002/bte2.20240036

[82] Zhao J, Han X, Wu Y, Wang Z, Burke AF. Opportunities and challenges in transformer neural networks for battery state estimation: Charge, health, lifetime, and safety. J Energy Chem. 2025;102:463–496. https://doi.org/10.1016/j.jechem.2024.11.011

[83] Zhao Y, Guo H, Guo X. Lithium-Ion Battery State-of-Health Estimation Method Based on Hierarchical Convolution and Multichannel Interactive Dense Transformer Network. IEEE Trans Instrum Meas. 2025;74:1–14. https://doi.org/10.1109/tim.2025.3576954

[84] Wang F, Zhai Z, Zhao Z, Di Y, Chen X. Physics-informed neural network for lithium-ion battery degradation stable modeling and prognosis. Nat Commun. 2024;15(1):4332. https://doi.org/10.1038/s41467-024-48779-z

[85] Amiri MN, Håkansson A, Burheim OS, Lamb JJ. Lithium-ion battery digitalization: Combining physics-based models and machine learning. Renew Sustain Energy Rev. 2024;200:114577. https://doi.org/10.1016/j.rser.2024.114577

[86] Singh S, Ebongue YE, Rezaei S, Birke KP. Hybrid Modeling of Lithium-Ion Battery: Physics-Informed Neural Network for Battery State Estimation. Batteries. 2023;9(6):301. https://doi.org/10.3390/batteries9060301

[87] Kohtz S, Xu Y, Zheng Z, Wang P. Physics-informed machine learning model for battery state of health prognostics using partial charging segments. Mech Syst Signal Process. 2022;172:109002. https://doi.org/10.1016/j.ymssp.2022.109002

[88] Wen P, Ye ZS, Li Y, Chen S, Xie P, Zhao S. Physics-Informed Neural Networks for Prognostics and Health Management of Lithium-Ion Batteries. IEEE Trans Intell Veh. 2024;9(1):2276–2289. https://doi.org/10.1109/tiv.2023.3315548

[89] Deng Y, Du C, Ren Z. A Novel Method for Estimating the State of Health of Lithium-Ion Batteries Based on Physics-Informed Neural Network. Batteries. 2025;11(2):49. https://doi.org/10.3390/batteries11020049

[90] Wei Y, Liu K, Rui J, Zhao Q. Integrating electrochemical-thermal-mechanical physical informed neural network framework for lithium-ion batteries state of health estimation. Energy AI. 2026;24:100713. https://doi.org/10.1016/j.egyai.2026.100713

[91] Yu Z, Liu J, Lu Y, Feng C, Li L, Wu Q. Combined EKF–LSTM algorithm-based enhanced state-of-charge estimation for energy storage container cells. J Power Electron. 2024;24(8):1329–1339. https://doi.org/10.1007/s43236-024-00801-9

[92] Wang S, Ou K, Zhang W, Wang YX. A State-of-Charge and State-of-Health Joint Estimation Method of Lithium-Ion Battery Based on Temperature-Dependent Extended Kalman Filter and Deep Learning. IEEE Trans Ind Electron. 2025;72(1):570–579. https://doi.org/10.1109/tie.2024.3409912

[93] Zhao H, Liao C, Zhang C, Wang L, Wang L. State-of-charge estimation of lithium-ion battery: Joint long short-term memory network and adaptive extended Kalman filter online estimation algorithm. J Power Sources. 2024;604:234451. https://doi.org/10.1016/j.jpowsour.2024.234451

[94] Li W, Rentemeister M, Badeda J, Jöst D, Schulte D, Sauer DU. Digital twin for battery systems: Cloud battery management system

with online state-of-charge and state-of-health estimation. J Energy Storage. 2020;30:101557. https://doi.org/10.1016/j.est.2020.101557

[95] Naseri F, Gil S, Barbu C, Cetkin E, Yarimca G, Jensen AC, et al. Digital twin of electric vehicle battery systems: Comprehensive review of the use cases, requirements, and platforms. Renew Sustain Energy Rev. 2023;179:113280. https://doi.org/10.1016/j.rser.2023.113280

[96] Kaleli AR, Türkkan A. ESTIMATION OF ELECTRIC VEHICLE MULTIPLE PACKAGE LITHIUM-ION BATTERY STATE OF CHARGE USING AN EXTENDED MACHINE LEARNING. Uludag Univ J Fac Eng. 2025;30(1):231–244. https://doi.org/10.17482/uumfd.1595646

[97] Eaty NDKM, Bagade P. Digital twin for electric vehicle battery management with incremental learning. Expert Syst Appl. 2023;229:120444. https://doi.org/10.1016/j.eswa.2023.120444

[98] Kim E, Jung S. Battery State of Health Estimation Methods: Implementation and Comparison of 11 Algorithms. IEEE Access. 2025;13:55599–55615. https://doi.org/10.1109/access.2025.3541631

[99] Pradhan SK, Chakraborty B. Battery management strategies: An essential review for battery state of health monitoring techniques. J Energy Storage. 2022;51:104427. https://doi.org/10.1016/j.est.2022.104427

[100] Yao L, Xu S, Tang A, Zhou F, Hou J, Xiao Y, Fu Z. A Review of Lithium-Ion Battery State of Health Estimation and Prediction Methods. World Electr Veh J. 2021;12(3):113. https://doi.org/10.3390/wevj12030113

[101] Meng J, Ricco M, Luo G, Swierczynski M, Stroe DI, Stroe AI, et al. An Overview and Comparison of Online Implementable SOC Estimation Methods for Lithium-Ion Battery. IEEE Trans Ind Appl. 2018;54(2):1583–1591. https://doi.org/10.1109/tia.2017.2775179

[102] Liu H, Li C, Hu X, Li J, Zhang K, Xie Y, et al. Multi-modal framework for battery state of health evaluation using open-source electric vehicle data. Nat Commun. 2025;16(1):1137. https://doi.org/10.1038/s41467-025-56485-7

[103] Lan T, Gao ZW, Yin H, Liu Y. A Sensor-Fault-Estimation Method for Lithium-Ion Batteries in Electric Vehicles. Sensors. 2023;23(18):7737. https://doi.org/10.3390/s23187737

[104] Yi B, Du X, Zhang J, Wu X, Hu Q, Jiang W, Hu X, Song Z. Bias-Compensated State of Charge and State of Health Joint Estimation for Lithium Iron Phosphate Batteries. IEEE Trans Power Electron. 2025;40(2):3033–3042. https://doi.org/10.1109/TPEL.2024.3492714

[105] Berecibar M, Garmendia M, Gandiaga I, Crego J, Villarreal I. State of health estimation algorithm of LiFePO4 battery packs based on differential voltage curves for battery management system application. Energy. 2016;103:784–796. https://doi.org/10.1016/j.energy.2016.02.163

[106] Badfar M, Yildirim M, Chinnam RB. State-of-charge estimation across battery chemistries: A novel regression-based method and insights from unsupervised domain adaptation. J Power Sources. 2025;628:235760. https://doi.org/10.1016/j.jpowsour.2024.235760

[107] Qin T, Zeng S, Guo J, Skaf Z. A Rest Time-Based Prognostic Framework for State of Health Estimation of Lithium-Ion Batteries with Regeneration Phenomena. Energies. 2016;9(11):896. https://doi.org/10.3390/en9110896

[108] Xu X, Yu C, Tang S, Sun X, Si X, Wu L. State-of-Health Estimation for Lithium-Ion Batteries Based on Wiener Process With Modeling the Relaxation Effect. IEEE Access. 2019;7:105186–105201. https://doi.org/10.1109/access.2019.2923095

[109] Pau DP, Aniballi A. Tiny Machine Learning Battery State-of-Charge Estimation Hardware Accelerated. Appl Sci. 2024;14(14):6240. https://doi.org/10.3390/app14146240

[110] Simon N, Peszleg R. Comparative Analysis of Electric Vehicle Energy Consumption in Urban and Highway Environments Using CAN-Based Data Collection. Engineering Perspective. 2025;5(1st Future of Vehicles Conf.):8–13. https://doi.org/10.64808/engineeringperspective.1795030

[111] Gou J, Yu B, Maybank SJ, Tao D. Knowledge Distillation: A Survey. Int J Comput Vis. 2021;129(6):1789–1819. https://doi.org/10.1007/s11263-021-01453-z

[112] Falai A, Giuliacci TA, Misul DA, Anselma PG. Reducing the Computational Cost for Artificial Intelligence-Based Battery State-of-Health Estimation in Charging Events. Batteries. 2022;8(11):209. https://doi.org/10.3390/batteries8110209

[113] Liu K, Shang Y, Ouyang Q, Widanage WD. A Data-Driven Approach With Uncertainty Quantification for Predicting Future Capacities and Remaining Useful Life of Lithium-ion Battery. IEEE Trans Ind Electron. 2021;68(4):3170–3180. https://doi.org/10.1109/tie.2020.2973876

[114] Raghavan A, Kiesel P, Sommer LW, Schwartz J, Lochbaum A, Hegyi A, et al. Embedded fiber-optic sensing for accurate internal monitoring of cell state in advanced battery management systems part 1: Cell embedding method and performance. J Power Sources. 2017;341:466–473. https://doi.org/10.1016/j.jpowsour.2016.11.104

[115] Li Y, Wang L, Song Y, Wang W, Lin C, He X. Functional Optical Fiber Sensors Detecting Imperceptible Physical/Chemical Changes for Smart Batteries. Nano-Micro Lett. 2024;16(1):154. https://doi.org/10.1007/s40820-024-01374-9

[116] Moser J, Rom W, Aichinger G, Kron V, Tuljapure PA, Ratz F, et al. Use of Lithium-Ion Batteries from Electric Vehicles for Second-Life Applications: Technical, Legal, and Economic Perspectives. World Electr Veh J. 2026;17(2):66. https://doi.org/10.3390/wevj17020066

[117] European Parliament and Council of the European Union. Regulation (EU) 2024/1257 of the European Parliament and of the Council of 24 April 2024 on type-approval of motor vehicles and engines and of systems, components and separate technical units intended for such vehicles, with respect to their emissions and battery durability (Euro 7). Off J Eur Union. 2024;2024/1257. https://eur-lex.europa.eu/eli/reg/2024/1257/oj